

Figure S1: Additional data related to Figure 1 and 2. Anatomy of the four paired pPAM neurons and coverage of pPAM neurons revealed by clonal analysis from the driver strains R30G08, R58E02 and R64H06

The pPAM cluster consists of four paired neurons, named pPAM1-4. Shown are frontal views of Z-projections on the mushroom body using anti-GFP (green) and anti-ChAT/FasII (magenta) antibodies. From left to right, the first column shows a projection of the mushroom body region; the second column shows the respective green

channel only; the third and fourth columns present detailed views of the ipsi- and contralateral medial lobe, respectively; the rightmost column depicts the ipsilateral innervation in the protocerebrum. Preparations were obtained using the flp-out technique from the driver strains R30G08 (for pPAM1 and pPAM3) and R64H06 (for pPAM2 and pPAM4). Similar morphology was found for all clones of a given neuron for the three Gal4 lines.

All four neurons have their cell body located in the anterior medial part of the brain. The primary neurite projects posterior up to an area medial of the base of the vertical lobe. Here, the primary neurite splits into two secondary branches. The first branch projects dorsally to form postsynaptic structures in the dorsal protocerebrum. The second branch runs basomedial to innervate the medial lobe ipsilaterally. From here, a single projection is crossing the midline to innervate the contralateral medial lobe in the same tile. Based on the gross anatomy of the medial lobe innervation, presynaptic structures (and some postsynaptic as well) are very likely. Irrespective of these general features, each pPAM neuron is individually identifiable:

(A-E) The pPAM1 neuron innervates the medial lobe most laterally compared to all other pPAM neurons, and is largely presynaptic in this region. Its postsynaptic innervation is not only restricted to an area medial to the vertical lobe of the mushroom body but also includes areas of the dorsolateral protocerebrum, further lateral of the vertical lobe. The shown clone is derived from the R30G08 driver strain.

(F-J) The pPAM2 neuron innervates the basal tip of the medial lobe, and is largely presynaptic in this region. Its postsynaptic innervation is restricted to the medial part of the brain next to the vertical lobe. In several cases pPAM2 clones showed a second or even a third presynaptic branch that crossed the midline more dorsally than the one innervating the medial lobes; these ended in the dorsomedial part of the contralateral brain by forming a small number of synaptic boutons. The shown clone is derived from the R64H06 driver strain.

(K-O) The pPAM3 neuron innervates the dorsal tip of the medial lobe, and is largely presynaptic in this region. Its postsynaptic arborization includes the medial part of the ipsilateral brain in a more widespread fashion, and more dorsally compared to pPAM2. The shown clone is derived from the R30G08 driver strain.

(P-T) The pPAM4 neuron innervates the very medial part of the medial lobe, and is largely presynaptic in this region. Its postsynaptic innervation is restricted to the most dorsomedial and basomedial protocerebrum. The shown clone is derived from the R64H06 driver strain.

Scale bars: 25 μ m.

(U-AF) All images show Z-projections of frontal views onto the larval brain. Clones of pPAM neurons are labeled by anti-GFP (green); anti-ChAT/FasII antibodies are used to visualize neuropil structures/axonal tracts (magenta). Typically, clones are obtained at frequencies of around 10% (solid green lines). In contrast, clones for the pPAM2 neuron in the driver strains R30G08 and R58E02 were yielded at much lower frequencies (solid grey line). In these two driver strains the pPAM2 neuron therefore does not show in the full expression pattern (note that in Figure 2D and E the pPAM2 tile is spared). Across the large number of animals involved in behavioral testing such low-probability expression is without measurable consequence, as the larvae in our assay behave independently of each other [S1].

(U, V, W, X) Single cell clones from R30G08 were regularly found for the pPAM1 and pPAM3 neuron (solid green lines), but only rarely for pPAM2 (solid grey line).

(Y, Z, AA, AB) Clones from R58E02 regularly yield the pPAM1, pPAM3, and pPAM4 neuron (solid green line), but only rarely pPAM2 (solid grey line). Note that (Z) shows a double-cell clone of the pPAM2 neuron in both hemispheres. Asterisks highlight the location of the four different subunits of the medial lobe in V and Z.

(AC, AD, AE, AF) Clones from R64H06 are regularly obtained for all four pPAM neurons (solid green line). Note that (AE) shows a double-cell clone of the pPAM3 neuron in both hemispheres. Scale bars: 50 μ m.

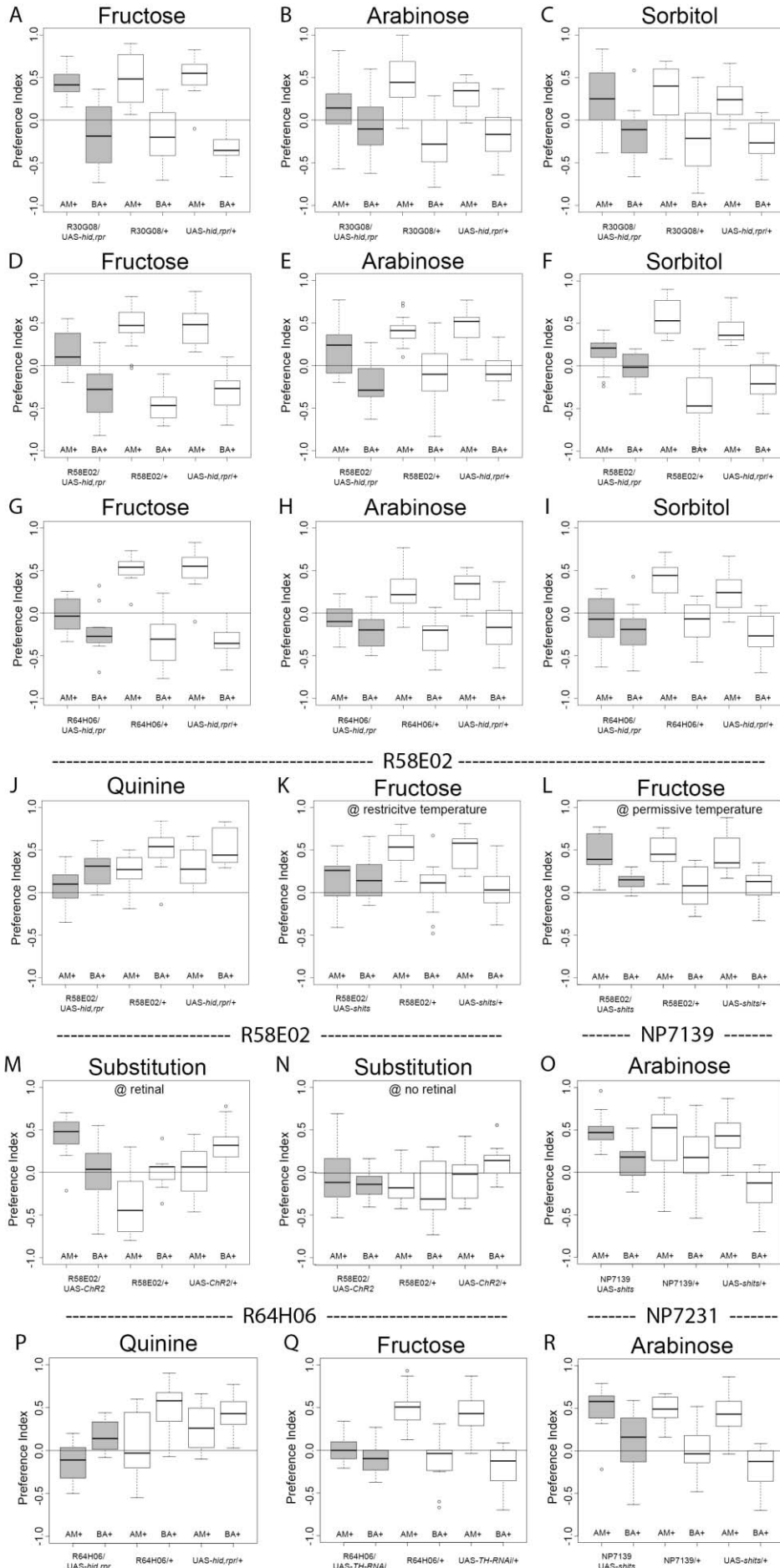
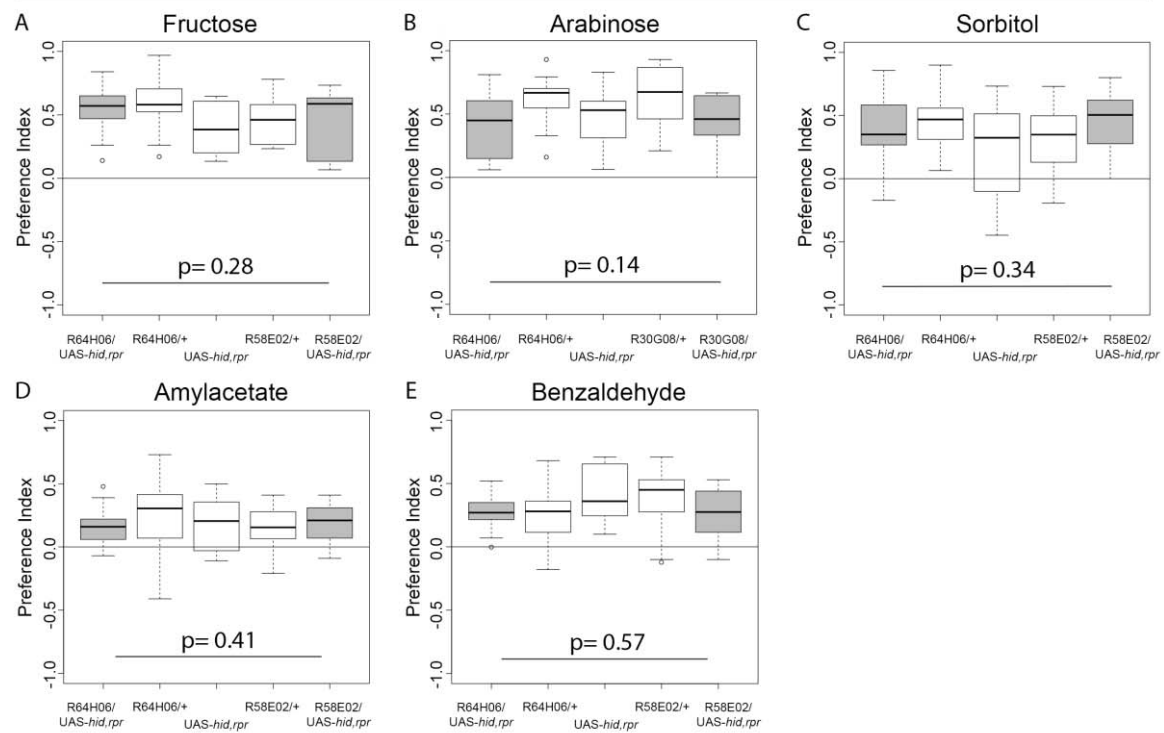


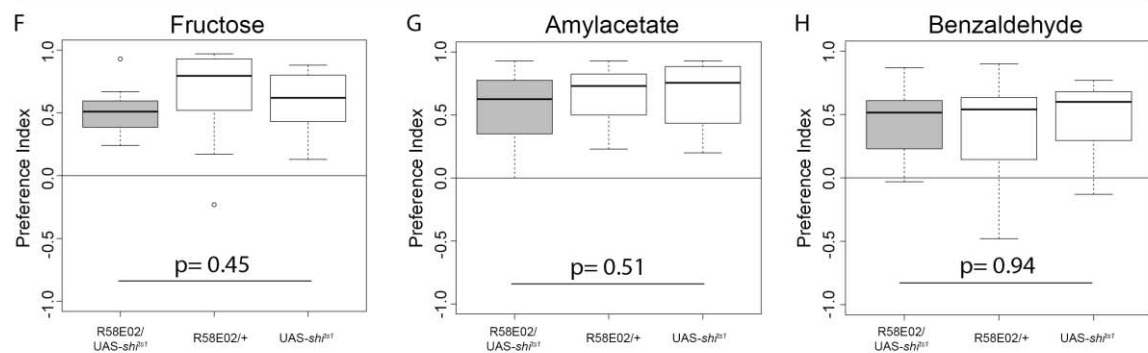
Figure S2: Additional data related to Figure 3. Preference indices

Preference Indices of the reciprocally trained groups underlying the associative Performance Indices shown in Figure 3. Preference Indices are measured either after the odor AM was paired with the respective reinforcer (e.g. AM+, left boxes for each genotype) or after the odor BA was paired with the reinforcer (e.g. BA+, right boxes). Positive values indicate approach towards AM, negative values indicate approach towards BA. Differences in preference between reciprocally trained groups indicate associative memory.

Cell ablation experiments



Blockage of neuronal output (measured at restrictive temperature)



TH knock-down via UAS-TH-RNAi using the driver line R64H06

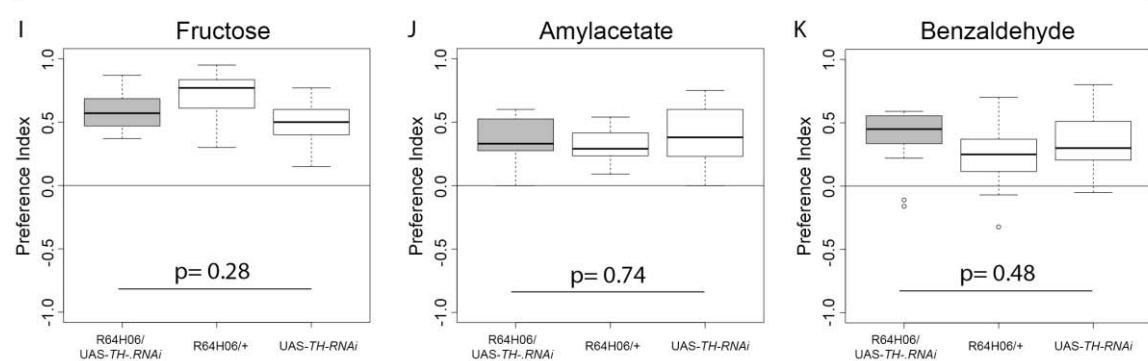


Figure S3: Additional data related to Figure 3. Manipulation of pPAM neurons leaves task-relevant sensory-motor faculties intact

Gustatory preference of experimentally naïve animals towards all three sugar rewards (A: fructose, B: arabinose, and C: sorbitol, respectively) is compared for those experimental groups that did show defects in the respective learning experiment upon ablation of pPAM neurons (see Figure 3A-K) and their respective genetic controls.

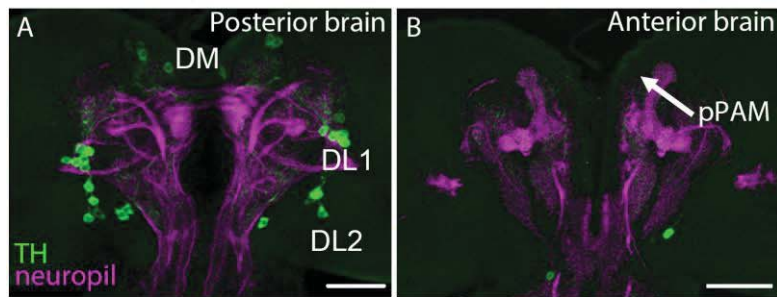
Likewise, in D and E the olfactory preference of experimentally naïve animals towards the to-be-associated odors AM (D) and BA (E) is shown.

In F-H the preference of experimentally naïve animals for the to-be-associated stimuli (fructose, AM, BA) upon blocking synaptic output from pPAM1,3,4 in the R58E02 driver strain (see Figure 3N) is shown.

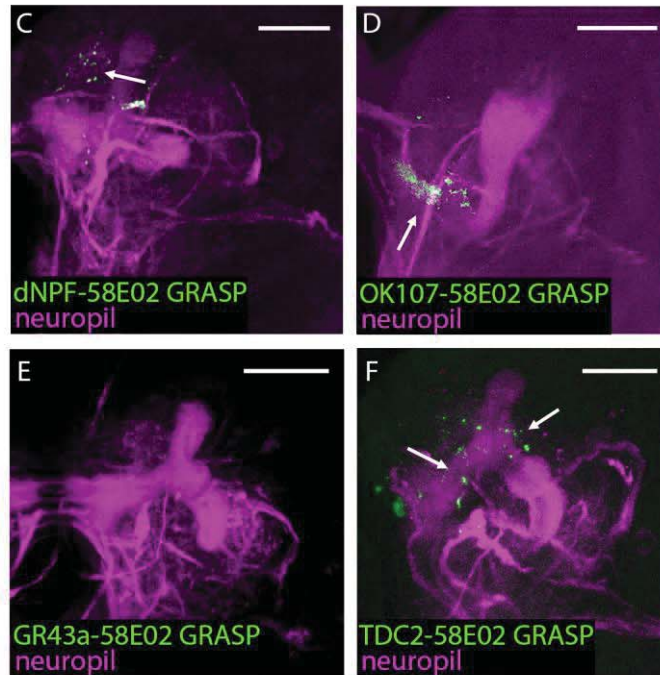
In I-K the preference of experimentally naïve animals for the to-be-associated stimuli (fructose, AM, BA) upon expression of UAS-TH-RNAi in the entire pPAM cluster via the R64H06 driver strain (see Figure 3Q) is shown.

In none of the cases do differences in preference reveal ($p > 0.05$ in Kruskal-Wallis tests), arguing that the defects in learning shown in Figure 3 are not secondary to defects in task-relevant sensory motor faculties.

----- R64H06/UAS-hid,rpr -----



----- GRASP experiments -----



--- Comparison of adult and larval expression pattern ---

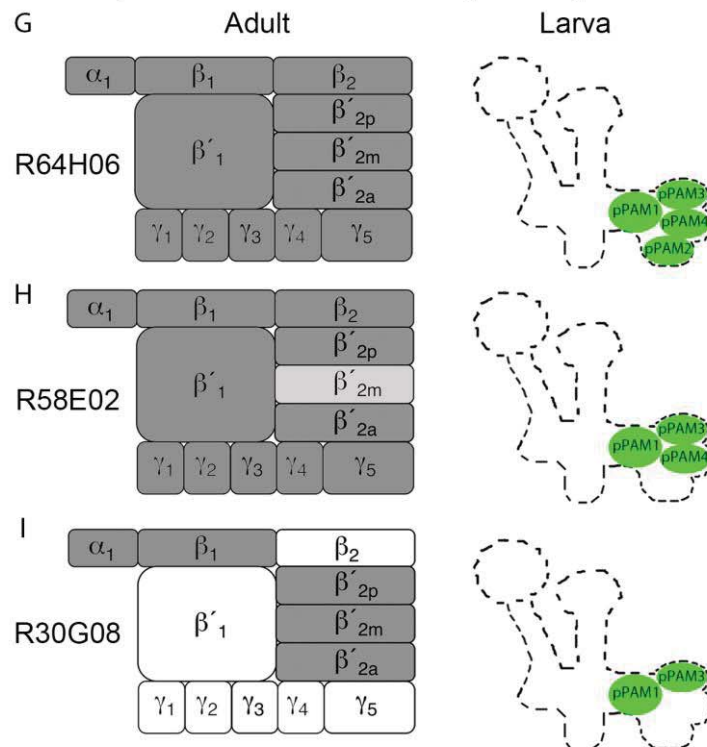


Figure S4: Additional data related to Figure 3. Verification of genetically induced cell ablation, identification of potential synaptic connections of pPAM neurons as judged by GFP reconstitution across synaptic partners (GRASP), and comparison of adult and larval expression patterns

(A and B) R64H06/UAS-*hid,rpr* labeled with anti-TH (to visualize potential dopaminergic neurons, green) and anti-ChAT/FasII antibodies (to reveal neuropil structures/axonal tracts, magenta). (A) Likely dopaminergic neurons in the posterior half of the brain are not altered and the three previously known clusters DL1, DL2, and DM are visible. (B) In the anterior half of the brain all four pairs of the pPAM cluster neurons are specifically ablated (arrow). Scale bars: 25 μ m.

(C–F) Partial Z-projection of frontal views for one hemisphere of larval brains of R58E02-LexA, LexAop-mCD4::GFP11; UAS-mCD4::GFP1-10 crossed with dNPF-Gal4 (C), OK107-Gal4 (D), GR43a-Gal4 (E) or TDC2-Gal4 (F), respectively. Reconstituted GFP is visualized in green; the neuropil/axonal tracts are visualized by anti-ChAT/FasII staining (magenta). The pPAM1,3,4 neurons as covered by the R58E02 LexA driver are in close proximity to neurons included in neuropeptide F positive neurons of the dNPF-Gal4 driver (C, arrow), mushroom body Kenyon cells included in the OK107-Gal4 expression pattern (D, arrow), and tyraminerpic/octopaminergic neurons included in the TDC2-Gal4 expression pattern (F, arrows). No GRASP signal was detectable when using GR43a-Gal4 together with R58E02-LexA (E). Scale bars: 50 μ m.

(G–I) Comparison of the adult (left) and larval (right) innervation of the mushroom body lobes by the driver strains R64H06, R58E02 and R30G08. R64H06 and R58E02 label nearly the entire larval medial lobe and show a similarly broad innervation at the adult stage. R30G08 innervation is more limited at both stages. Also note the higher number of medial-lobe mushroom body subunits and related PAM neurons in adults (12 subunits and about 120 PAM neurons, rather than 4 subunits and 4 pPAM neurons in the case of larvae). This prompts the tempting speculation that adults can perceive, classify and distinguish rewarding stimuli in more different types than larvae.

Supplemental Experimental Procedures

Fly strains

Fly strains were reared on standard *Drosophila* medium at 25°C with a 14/10 h light/dark cycle [S2,S3]. For the GRASP experiments the following strains were used: R58E02-LexA/CyO, LexAop-*mCD4::GFP11*, UAS-*mCD4::GFP1-10/TM6B* virgins were crossed to dNPF-Gal4, OK107-Gal4, GR43a-Gal4 or TDC2-Gal4, respectively (Bloomington Drosophila Stock Center No.: 854, 9313, 25682 and 57637) [S4].

GRASP

In the F1 generation of these crosses, larval brains were dissected and stained using the described standard protocol (for details see section “Immunostaining”) [S2].

Antibodies

To analyze the larval expression patterns in the different GRASP experiments two different mouse antibodies for staining the cholinergic neuropil (ChAT4B1; DSHB, Iowa City, IA, 1:150) and axonal tracts (1d4 anti-Fasciclin II; DSHB, Iowa City, IA; 1:50) were applied [S2]. As secondary antibody a goat anti-mouse IgG Alexa Fluor 647 (A21235, Molecular Probes, 1:200) was used. The reconstituted GFP expression was analyzed based on its strong endogenous signal (shown in Figure S3). There was no difference detectable between the two kinds of GFP signal.

Sensory acuity tests

Sensory tests were performed using standard methods [S3,S5,S6]. For olfactory acuity tests, 2.5% agarose solution (Sigma Aldrich Cat. No.: A5093; CAS No.: 9012-36-6) was boiled in a microwave and filled as a thin layer into Petri dishes (85 mm diameter, Cat. No.: 82.1472, Sarstedt, Nümbrecht). After cooling, closed Petri dishes were kept at room temperature and were used on the same day. For gustatory acuity tests, the agarose dishes were prepared in the same way, except that after cooling the agarose was removed from half of the plate. The empty half was filled by 2.5% agarose solution in addition containing 2 M fructose, 2 M arabinose, or 2 M sorbitol.

For olfactory acuity assays, 10 µl of either pure benzaldehyde or diluted amyl acetate (1:250 in paraffin oil) were loaded into a custom made Teflon container. Olfactory preferences were tested by placing 30 larvae in the middle of the Petri dish with an odor-filled Teflon container on one side and an empty container on the other side (AIR). Larvae were then counted after 5 minutes as being located either on the odor side, the no-odor side, or a middle neutral zone (a stripe of about 10 mm width running vertically in the middle of the plate). For gustatory acuity tests, 30 larvae were put in the middle of a Petri dish that contained pure agarose on one side and agarose plus a gustatory stimulus (fructose, arabinose or sorbitol) on the other side. Larvae were counted after 5 minutes as being located on either the sugar side, the no-sugar side, or a middle neutral side (an area of about 10 mm width running vertically in the middle of the plate).

The indices for sensory acuity were then calculated as follows:

$$\text{Preference Index} = (\# \text{ ODOR} - \# \text{ AIR}) / \# \text{ TOTAL}$$

Positive Preference Indices therefore indicate attraction of the particular odor (amyl acetate or benzaldehyde, as indicated above each panel of Figure S4).

$$\text{Preference Index} = (\# \text{ SUGAR} - \# \text{ PURE AGAROSE}) / \# \text{ TOTAL}$$

Positive Preference Indices therefore indicate attraction of the particular sugar (fructose, arabinose, or sorbitol, as indicated above each panel of Figure S4).

Supplemental References

- S1. Niewalda, T., Jeske, I., Michels, B., and Gerber, B. (2014). 'Peer pressure' in larval *Drosophila*? *Biol Open* 3, 575-582.
- S2. Selcho, M., Pauls, D., Han, K.A., Stocker, R.F., and Thum, A.S. (2009). The role of dopamine in *Drosophila* larval classical olfactory conditioning. *PLoS One* 4, e5897.
- S3. Apostolopoulou, A.A., Widmann, A., Rohwedder A., Pfitzenmaier J.E., and Thum, A.S. (2013). Appetitive associative olfactory learning in *Drosophila* larvae. *J Vis Exp* 72, pii: 4334.
- S4. Liu, C., Placais, P.Y., Yamagata, N., Pfeiffer, B.D., Aso, Y., Friedrich, A.B., Siwanowicz, I., Rubin, G.M., Preat, T., and Tanimoto, H. (2012). A subset of dopamine neurons signals reward for odour memory in *Drosophila*. *Nature* 488, 512-516.
- S5. Gerber, B., and Stocker, R.F. (2007). The *Drosophila* larva as a model for studying chemosensation and chemosensory learning: a review. *Chem. Sens.* 32, 65-89.
- S6. Hendel, T., Michels, B., Neuser, K., Schipanski, A., Kaun, K., Sokolowski, M.B., Marohn, F., Michel, R., Heisenberg, M., and Gerber, B. (2005). The carrot, not the stick: appetitive rather than aversive gustatory stimuli support associative olfactory learning in individually assayed *Drosophila* larvae. *J Comp Physiol A Neuroethol Sens Neural Behav Physiol* 191, 265-279.